Unstable Shastry-Sutherland phase in Ce_2Pd_2Sn

J. G. Sereni,[1] M. Gómez Berisso,[1] A. Braghta,[2,3] G. Schmerber,[3] and J. P. Kappler[3]
[1]*División Bajas Temperaturas, Centro Atómico Bariloche (CNEA), 8400 San Carlos Bariloche, Argentina*
[2]*Département de Physique, Université de Guelma, 24000 Guelma, Algeria*
[3]*IPCMS, UMR 7504 CNRS-ULP, 23 rue de Loess, Boîte Postale 43, 67084 Strasbourg Cedex 2, France*
(Received 7 April 2009; revised manuscript received 7 July 2009; published 31 July 2009)

Thermal (C_P), magnetic (M and χ_{ac}), and transport (ρ) measurements on Ce_2Pd_2Sn are reported. High-temperature properties are well described by the presence of two excited crystal-field levels at (65 ± 5) K and (230 ± 20) K, with negligible hybridization (Kondo) effects. According to literature, two transitions were observed at $T_M=4.8$ K and $T_C=2.1$ K, respectively. The upper transition cannot be considered as a standard antiferromagnetic because of frustration effects in a triangular network of Ce atoms and the positive sign of the paramagnetic temperature $\theta_P^{LT}=4.4$ K. The nature of the intermediated phase is described accounting for the formation of ferromagnetic (F) Ce dimers disposed in a quasi-two-dimensional square lattice, resembling a Shastry-Sutherland pattern. According to hysteretic features in $\rho(T)$ and $\chi_{ac}(T)$, the lower F transition is of first order, with C_P $(T<T_C)$ revealing a gap of anisotropy $E_g\approx7$ K.

DOI: 10.1103/PhysRevB.80.024428 PACS number(s): 75.20.Hr, 71.27.+a, 75.30.Kz, 75.10.−b

I. INTRODUCTION

The competition between different phases is resolved according to thermodynamic laws, with the configurational entropy as an important factor to define the state of lower free energy (G) as the temperature is reduced. However, complex or metastable phases may occur since roughness in the G function of real systems may produce relative minima which become relevant. At the transition temperature, where the G minimum broadens according to the Ginsburg-Landau theory, the effect of exotic minima is favored. Within that context, there are nontrivial types of orders, such as frustration, incommensurability, glasses, or even superconductivity related to quantum critical points, which may occur when the system does not accede directly to an absolute minimum of energy.

The search of experimental examples where these conditions are realized is an important task in current investigations. The highest probability to find the mentioned conditions occurs in systems exhibiting multiple phase transitions because that situation reveals the competition between different configurations of comparable energy. According to literature, the rare-earth-based ternaries with the formula R_2T_2X are suitable candidates for such a purpose, as it was demonstrated by the study of the $Yb_2Pd_2(In,Sn)$ system.[1] In this In/Sn doped alloy, the stoichiometric limits are nonmagnetic heavy Fermion compounds while incipient magnetic order shows up at intermediate In/Sn substitution.

Crystal chemistry and magnetic properties of R_2T_2X compounds [with R=Ln (Refs. 2 and 3) and Ac,[4] T=Transition Metals of the VIII group[2,5,6] and X=early p metals[5]] have been investigated over the past two decades motivated by their peculiar crystalline structure and magnetic behaviors. Their tetragonal Mo_2FeB_2-type structure[4] is strongly anisotropic and can be described as successive "$T+X$" (at $z=0$) and "R" (at $z=1/2$) layers.

$Ce_{2\pm x}Pd_{2\pm y}X_{1\mp z}$ (with $x+y+z=0$) show an extended range of solubility. This favors that different types of magnetic configurations with similar energy compete for the formation of different phases. In fact, by tuning small excess/deficit of the components (x,y,z) one can drive these compounds between ferromagnetic (F) and antiferromagnetic (AF) orders. In $Ce_{2\pm x}Pd_{2\pm y}In_{1\pm z}$ alloys,[3] for example, the existence of two magnetic branches (namely, F and AF) was determined in the ternary phase diagram.

In the case of $Ce_2Pd_{2+x}Sn_{1-x}$ stannide[7] two transitions at $T_N=4.7$ K and $T_C=3.0$ K were reported. Neutron diffraction experiments[8] revealed a modulated character of this intermediate phase, with the local moments pointing in the "c" direction and an incommensurate propagation vector $[qx]$ changes from 0.11 (at 4.2 K) to 0.077 (at 2.8 K). At that temperature it suddenly drops to $[qx=0]$, becoming ferromagnetic.

Despite these results there are some contradictory features in the low-temperature behavior of this compound. For example, it is unlikely to expect a standard AF behavior in a triangular network of magnetic atoms under geometrical frustration constraints. Furthermore, the reported value of the paramagnetic temperature θ_P^{LT} is positive, and practically coincide with the upper magnetic transition temperature.[9] These properties impose a revision of the proposed AF character of that phase. For that reason we will label the upper transition as T_M instead of T_N like proposed in the literature.

In this paper we present a thorough investigation on thermal, magnetic, and transport properties between 0.5 K and room temperature on Ce_2Pd_2Sn. These results prove the local character of the Ce moments, provide insight into the knowledge of the nature of intermediate phase at $T_M>T>T_C$ and the ferromagnetic character of the ground state (GS).

II. EXPERIMENTAL DETAILS AND RESULTS

Since the magnetic properties of these compounds show a strong dependence on composition, we have chosen for this study a nearly stoichiometric sample with actual composition $Ce_{2.005}Pd_{1.988}Sn_{0.997}$ [after scanning electron microscopy (SEM)/energy dispersive x-ray analysis (EDAX) analysis] and a standard deviation of $\pm0.5\%$. Details of sample prepa-

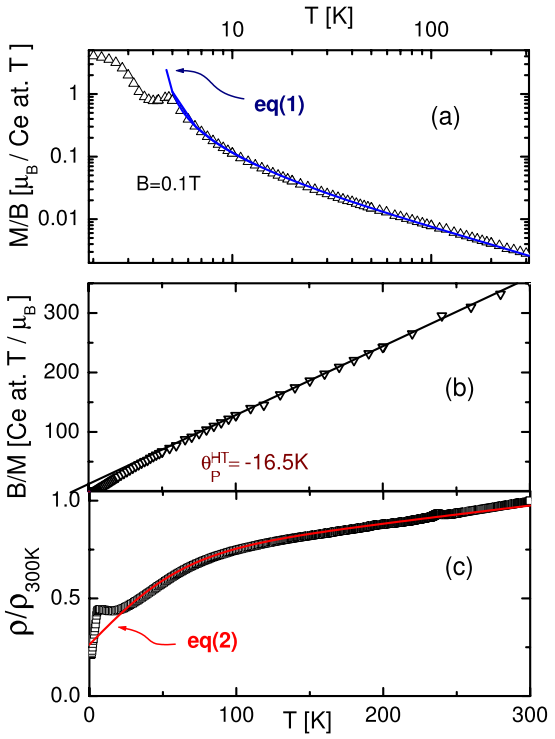

FIG. 1. (Color online) High-temperature properties of Ce_2Pd_2Sn. (a) Thermal dependence of field normalized magnetization M/B in a double logarithmic representation. (b) Inverse magnetization B/M, with $B=0.1$ T. Straight line represents the extrapolation from high temperature to extract θ_P^{HT}. (c) Temperature dependence of normalized electrical resistivity $\rho(T)/\rho_{300\ \mathrm{K}}$. Dashed curves in (a) and (c) are fits using Eqs. (1) and (2), respectively, see the text.

ration were described in a previous paper.[9] Lattice-parameters study confirmed the single phase character of the sample with Mo_2FeB_2-type structure. The respective lattice parameters are: $a=7.765$ Å and $c=3.902$ Å, with a $c/a=0.5026$ ratio. The standard deviation in the lattice-parameters determination is ± 0.002 Å.

Electrical resistivity was measured between 0.5 K and room temperature using a standard four probe technique with an LR700 bridge. Dc-magnetization measurements were carried out using a superconducting quantum interference device magnetometer operating between 2 and 300 K, and as a function of field up to 5 T. For ac susceptibility a lock-in amplifier was used operating at 1.28 kHz, with an excitation field of 1 Oe on compensated secondary coils in the range of 0.5–10 K. Specific heat was measured using the heat-pulse technique in a semiadiabatic He-3 calorimeter in the range between 0.5 and 20 K, at zero and applied magnetic fields up to 4 T.

A. High-temperature results

High-temperature dc magnetization M/B and electrical resistivity ρ results are presented in Fig. 1. The former is depicted as M/B vs T in a double logarithmic scale [Fig. 1(a)], while the latter was normalized to the room-temperature value $\rho_{300\ \mathrm{K}}$ [Fig. 1(c)]. Both curves are in good agreement with results obtained on similar samples.[7,10] Figure 1(b) shows the inverse of the magnetization B/M used to extract the high-temperature effective moment μ_{eff}^{HT} and paramagnetic Curie-Weiss temperature θ_P^{HT}.

$M(T)$ was measured up to room temperature with an applied field $B=0.1$ T. At $T_M=4.8$ K, it shows a cusp which was previously taken as an indication for an AF character of that transition. However, the divergent increase in $M/B(T \rightarrow T_I)$ with $T_I=4.4$ K, makes that argument uncertain. The analysis of these results can be done applying a simple formula:[11]

$$M/B = \sum_0^2 \mu_i^2 * \exp(-\Delta_i/T)/[(T-T_I)*Z], \qquad (1)$$

where μ_i are the effective moments of the ground state ($i=0$) and excited crystal-field (CF) levels ($i=1$ and 2, respectively). This high quality fit in such a wide range of temperature, using an equation that only takes into account the Boltzmann thermal occupation of the excited CF levels, indicates that those levels are very well defined in energy.

The values obtained by applying this formula are: $\mu_0=1.7\pm0.1\mu_B$, $\mu_1=1.9\pm0.1\mu_B$, and $\mu_2=2.48\pm0.15\mu_B$, and the respective CF splittings: $\Delta_1=65\pm4$ K and $\Delta_2=230\pm20$ K. Since at room temperature the upper CF level is not yet fully occupied, the value for a $J=5/2$ moment is not reached. Due to the simplicity of Eq. (1), where three nondiagonal Van Vleck terms are not taken into account, these values have only a qualitative character. The relevant information extracted from this fit for our study is: (i) with a CF splitting of $\Delta_1>60$ K, any influence of the excited CF levels can be excluded from the GS properties, (ii) such a good fit obtained using narrow CF excited levels excludes any significant "4*f*-band" hybridization effect, consequently (iii) $\Delta_1 \gg T_K$.

The inverse of the susceptibility B/M shows a Curie-Weiss behavior at high temperature [i.e., $T \geq 80$ K, see Fig. 1(b)] with an extrapolation for the paramagnetic Curie-Weiss temperature: $\theta_P^{HT}=-16.5$ K, in agreement with the literature.[7] However, below $T \approx 80$ K a negative curvature takes over as the thermal population of the excited CF levels decreases. This results in a positive value of the low-temperature extrapolation: $\theta_P^{LT} \rightarrow 4.4$ K [see Fig. 2(b)], in coincidence with the divergence at $T \rightarrow T_I$ in Eq. (1). The proximity of θ_P^{LT} to T_M is an evidence of a competition between different types of interactions, since the former is related to a F divergence and the latter to an AF-like cusp in $M(T)$.

$\rho(T)$ dependence can be described following the Matthiessen criterion: $\rho(T)=\rho_0+\rho_m(T)+\rho_{ph}(T)$, where ρ_0 is the residual resistivity, $\rho_m(T)$ the magnetic contribution and $\rho_{ph}(T)$ the phonon contribution to electronic scattering. Due to the mentioned negligible hybridization effects on the excited CF levels $\rho(T)$ is described very well by the simple expression,[12] as shown in Fig. 1(c):

$$\rho(T) = a + b*\tanh(T/D) + c*T, \qquad (2)$$

where $a=\rho_0$, $b*\tanh(T/D)=\rho_m$, and $c*T=\rho_{ph}(T)$. The most relevant parameter in this equation is D because it provides

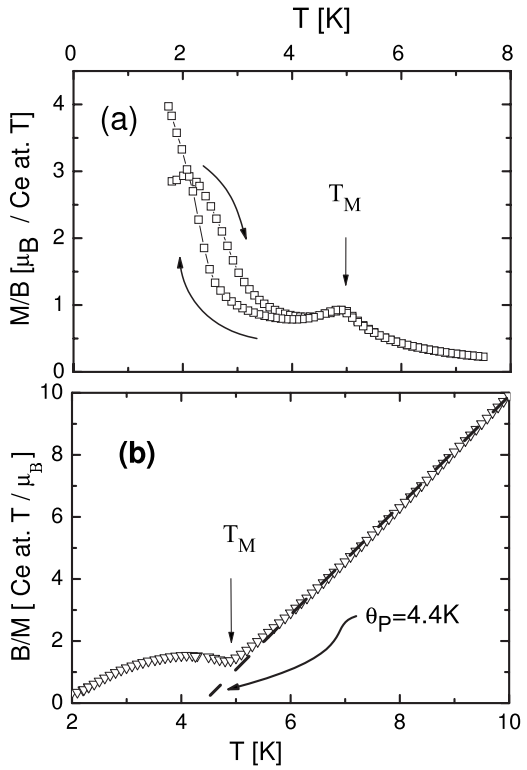

FIG. 2. (a) Comparison of magnetization results in field (B =5 mT) cooling and heating (after ZFC) processes. (b) Low-temperature inverse magnetization B/M, with B=0.1 T. Dashed line represents the extrapolation from high temperature to obtain θ_P^{LT}.

an estimative scale of energy for the dominant scattering center at intermediate temperature, which in this case corresponds to the first excited CF level Δ_1=63 K. The second CF excited level can be estimated at $\Delta_2 > 200$ K. These values are in good agreement with those extracted from $M/B(T)$.

B. Low-temperature results

As indicated by $M(T)$ results, the low-temperature behavior ($T<20$ K) of this compound is rather complex. Hence, some previous considerations are required to better understand the experimental results presented in this section. Since the AF molecular field (with $\theta_P^{HT}=-16.5$ K) turns to ferromagnetic ($\theta_P^{LT} \rightarrow 4.4$ K) below about 20 K, one may distinguish a correlated paramagnetic region for 20 K$>T>T_M$ respect to the canonical one occurring above 20 K. As mentioned before, despite of the cusp at $M(T_M)$, this upper transition is strongly affected by those F-type correlations. This situation persists in the intermediate phase ($T_M > T > T_C$) and it is only below T_C that the stable F ground state is established.

For 20 K$>T>T_M$, $\rho(T)$ shows a slight increase. Such an increase in $\rho(T \rightarrow T_M)$ might be attributed to Kondo effect, however, it is also observed above ferromagnetic transitions, such as, e.g., in GdPt.[13] In that case, the increase in $\rho(T \rightarrow T_C)$ arises from F fluctuations, precursors of the magnetic transition. Below T_M, $\rho(T)$ decreases without any sign of AF gap opening at the transition. At $T=T_C$, hysteretic effects are observed, which are practically suppressed by a field of nearly 0.2 T.

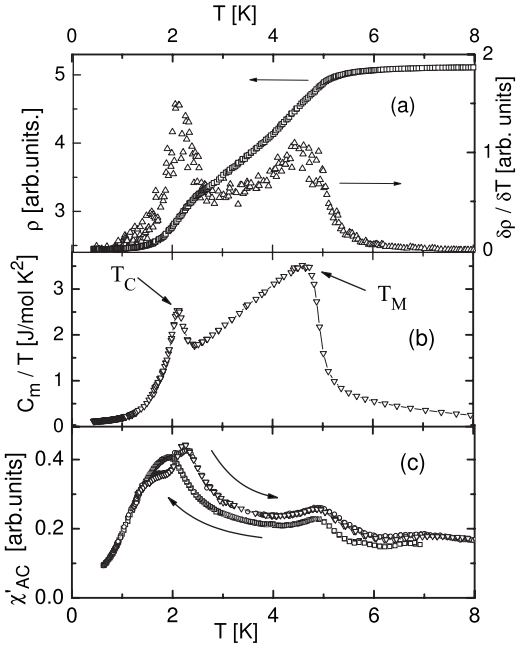

FIG. 3. (a) Low-temperature electrical resistivity (left axis) and its temperature derivative (right axis). (b) Magnetic contribution to specific heat divided by temperature showing the upper (modulated) T_M and the lower (f) transitions. (c) Ac susceptibility as a function of temperature in cooling and (two runs) on heating procedures.

Specific heat, $C_P(T)$, also shows an increasing contribution for $20>T>T_M$ [see Fig. 3(b)] arising from magnetic correlations precursors of T_M transition. Since this $C_P(T>T_M)$ tail contains important information about the nature of the related transition, it will be analyzed in detail in the discussion section.

1. Modulated phase ($T_M > T > T_C$)

$M(T)$ is certainly the most sensitive parameter to F correlations. The low-field (B=5 mT) magnetization results shown in Fig. 2(a) confirm the ambiguous behavior of the intermediate phase. The difference between cooling ($T\downarrow$) and heating ($T\uparrow$) processes is evident, especially below T_I =4.4 K($=\theta_P^{LT}$) which can be considered as a temperature of irreversibility. This means that the AF character proposed in the literature owing to the modulated magnetic structure is never properly established.

Both magnetic transitions are determined from $C_m/T(T)$ measurements by the respective jumps at T_M=4.8 K and T_C=2.1 K, respectively, as shown in Fig. 3(b). $C_m/T(T)$ is obtained after subtraction of phonon contribution using La_2Pd_2Sn as reference: $C_m/T=C_P/T-C_P/T(La_2Pd_2Sn)$. The $C_m(T)$ dependence for $T_M \geq T \geq T_C$ does not fit into the expected for a canonical AF, namely, $C_m(T) \propto T^3$. Instead, the observed dependence: $C_m(T)=0.5T^{2.25}$ is closer to that of a strongly anisotropic ferromagnet with $C_m(T) \propto T^{2.5}$.[14]

Ac-susceptibility χ_{ac} measurements, presented in Fig. 3(c), confirm these findings with an increasing signal below

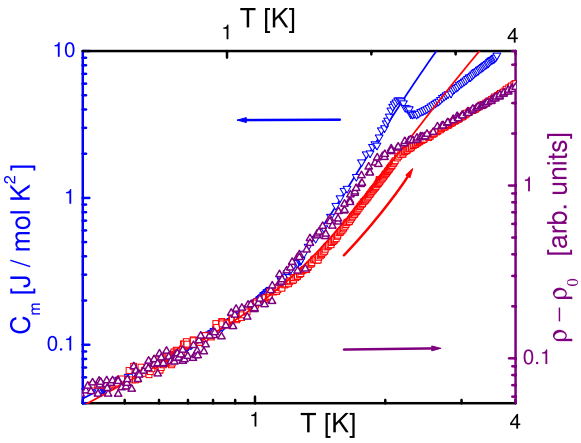

FIG. 4. (Color online) Comparison of T dependencies of magnetic specific heat (left axis) and electrical resistivity (right axis) of the F phase. Cooling and heating runs of resistivity show a hysteresis at T_C.

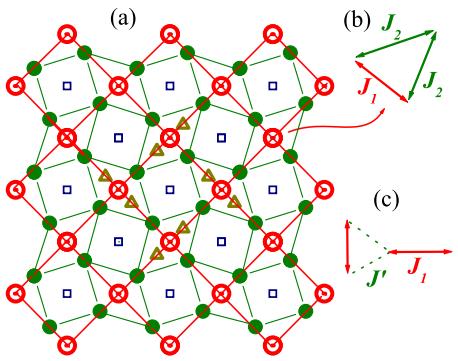

FIG. 5. (Color online) (a) Mo_2FeB_2-type structure showing Ce (green ●), Sn (blue □), and Pd (dark yellow △) atoms. Superposed is a schematic representation of a square lattice (red lines) built up by F dimers (⊙) with moments pointing in the "c" direction. (b) Magnetic interactions: J_1 (red) and J_2 (green), between Ce atoms on the "ab" plane. (c) Magnetic interactions J' (green dots) between neighboring dimers.

4 K and a maximum at T_C which depends on the cooling or heating process and confirm hysteretic behavior.

2. *Ferromagnetic phase* ($T < T_C$)

The hysteretic behavior between $T\downarrow$ (with χ_{ac}^{max} at $T \approx 1.9$ K) and $T\uparrow$ (with χ_{ac}^{max} at $T \approx 2.2$ K) indicates the first-order character of the ferromagnetic transition, see Fig. 3(c). However, the lower boundary of this hysteretic region is observed at ≈ 1.3 K and, in the heating process, a shoulder in $\chi_{ac}(T\uparrow)$ appears at $T \approx 1.5$ K. This anomaly can be attributed to a very small amount of ferromagnetic Ce_3Pd_5,[15] which is not even detected in $C_P(T)$ nor in $\rho(T)$ measurements.

Also the temperature dependence of the electrical resistivity shows hysteretic behavior between cooling and heating around T_C as it can be seen in Fig. 4. From specific heat results, the ferromagnetic transition occurs at $T_C = 2.1$ K with a sharp anomaly characteristic of first order type, which involves a small amount of latent heat.

Within the F phase, both $C_m(T)$ and $\rho_m(T)$ are very well described by their respective F-temperature dependencies containing an exponential factor due to the presence of a gap in the magnon spectrum, see Fig. 4. Those functions are[16]

$$C_m(T) = \gamma T + T^{3/2}[a + b\exp(-E_g/T)] \quad (3)$$

with $\gamma = 7$ mJ/mol K^2 confirming the absence of Kondo effect, and $E_g = 7.5$ K. The electrical resistivity is well described by:[17]

$$\rho(T) \propto T^{1/2}\exp(-E_g/T)[1 + cT/E_g + d(T/E_g)^2] \quad (4)$$

with a similar value for the gap: $E_g = 7.2$ K. The presence of this gap is a clear indication of the strong anisotropy of this system.

III. DISCUSSION

The strong local character of the "4f" orbital, as a well defined trivalent Ce atom, is concomitant with the absence hybridization (or Kondo) effect on ground and CF excited states. Within such a scenario, a F ground state is usually expected for Ce compounds.[18] Knowing that the twin compound $Ce_{2\pm x}Pd_{2\pm y}In_{1\pm z}$ modifies its magnetic structure with a slight variation in composition,[3] one should ask whether the intermediate phase is an exotic phase appearing under this special situation of competing exchange interactions. Thus, the formation of such a phase previous to the stabilization of the F-GS raises the question about the role of the atomic configuration in this peculiar crystalline structure together with the consequent steric distribution of magnetic interactions. Accordingly, modulated/incommensurate nature of the propagation vector hints for an exotic character of that phase. Therefore, its origin should be searched mainly taking into account its structural properties rather than only the electronic ones.

A. Structural properties

The structural disposition of R atoms in these compounds can be depicted as trigonal and tetragonal prisms, centered around "T" and "X" atoms, respectively, with the "R" atoms in noncentrosymmetric positions along the "c" direction. As a consequence of the trigonal disposition, there is a "one-to-one" correlation of magnetic properties between Ce_2T_2X compounds and the corresponding CeT binary compounds[19] with CrB- or FeB-type structures (both structured in trigonal prisms[20]). This results in an assembled mosaic of rhombuses and squares projected on the basal plane. While the rhombuses are rotated $\pi/2$ with respect to their four parent nearest neighbors (nn), the squares are rotated $\pi/4$ among them (see Fig. 5), mimicking a sort of "pinwheel" centered on the Sn-Sn column.

An important characteristic of this family of compounds is that the shortest $d_{R\text{-}R}$ spacing (i.e., the nearest R-R neighbors, Rnn) can be either in the c direction (2nn) or in the basal "ab" plane (1nn) depending on the "c/a" ratio of the lattice parameters. Values of $c/a < 0.5022$ favor the formation of "R" chains parallel to "c," like in U_2Ni_2In.[4] On the contrary, for larger "c/a" values there is only one R-R first

*R*nn lying on the basal plane. Their distance is the shorter diagonal of the rhombus polygon [see Fig. 5(a)] and separates two triangular prisms disposed in mirror position, centered on the Pd-Pd column.

In Ce_2Pd_2Sn, the ratio $c/a=0.5026$ indicates that the nn is only one atom lying on the $z=1/2$ plane. However, the difference with respect to the two next nn (in the "*c*" direction) is less than 1%: $d_{\text{Ce-1Ce}}=3.882$ Å and $d_{\text{Ce–2Ce}}=3.902$ Å, respectively. These two Ce-Ce spacings lie within the $3.7<d_{\text{Ce-Ce}}<4.0$ Å range where F-Ce dimers are placed,[19] including CePd.

B. Nature of the modulated phase

To evaluate the consequences of these structural characteristics on the magnetic properties, one has to take into account that the effective Ruderman-Kittel-Kasuya-Yoshida (RKKY) interaction depends on three parameters:

$$J_{eff}(r) = J_{ex} * \mathbb{S}(\mathbb{S}+1) * f_{\text{RKKY}}(r), \tag{5}$$

where J_{ex} is the intensity of the exchange interaction between *R*-nn atoms, $\mathbb{S}$ represents the magnetic spin and $f_{\text{RKKY}}(r)$ is the RKKY oscillatory function. One has to consider different values of J_{ex} corresponding to each type of neighbor: J_1 and J_2 for the respective nn (one) and the next-nearest-neighbor (nnn) (four) neighbors on the "*ab*" plane, see Fig. 5(b). According to neutron measurements,[8] J_c connecting Ce atoms with those of the upper and lower plane is not relevant in this range of temperature.

Although this compound shows its upper magnetic transition at $T_M=4.8$ K, the presence of magnetic correlations is observed at much higher temperatures in the tail of $C_m(T>T_M)$ and the increase in $\rho(T<15$ K). These signs of incipient magnetic correlations within the paramagnetic phase contain important information about the nature of the transition itself since they contain the contribution of related precursors. Furthermore, strongly anisotropic or low-dimensional systems display a significant amount of entropy above the transition. The existence of such a correlated paramagnetic region in the compound under study is confirmed by the fact that it has to be heated at least up to ≈20 K for a zero-field-cooled (ZFC) process, otherwise traces of remanent magnetic contributions are detected afterwards.

A deeper analysis of $C_m(T)$ shows that the temperature dependence at $T>T_M$ is $C_m \propto 1/T^2$, in coincidence with the specific heat of $CoCs_3Br_5$ (Ref. 21) [see Fig. 6(a)], which is an archetype for a quadratic spin $\mathbb{S}_{eff}=1$ square lattice. Notice that not only the temperature dependence coincides but also their respective absolute values, provided that for Ce_2Pd_2Sn C_m is taken in "mol" units (i.e., 2 Ce atoms). Notice that the transition temperature of the model compound is scaled to compound under study. The jump of the specific heat also points in that direction, since in mean-field theory the jump of the specific heat at a magnetic transition is given by: $\Delta C_m=2.5R[(2\mathbb{S}_{eff}+1)^2-1]/[(2\mathbb{S}_{eff}+1)^2+1]$,[22] which for $\mathbb{S}_{eff}=1/2$ is $\Delta C_m=1.5R$, while for $\mathbb{S}_{eff}=1$ it becomes $\Delta C_m=2R$ like the measured value.

The magnetic entropy, computed as $\Delta S_m=\int C_m/TdT$, reaches the expected value $\Delta S_m=2R\ln 2$ for a doublet ground state at around 15 K (the prefactor 2 corresponds to two magnetic atoms per f.u.). As depicted in Fig. 6(b), the entropy gain reaches 80% of that value at $T=T_M=4.8$ K. This is a direct consequence of the low value of $T_K \approx 3.0$ K, which can be evaluated from $\Delta S_m(T)$ by applying the Desgranges-Schotte[23] criterion of $\Delta S_m(T=T_K) \cong 2/3R\ln 2$ for a nonordered system.

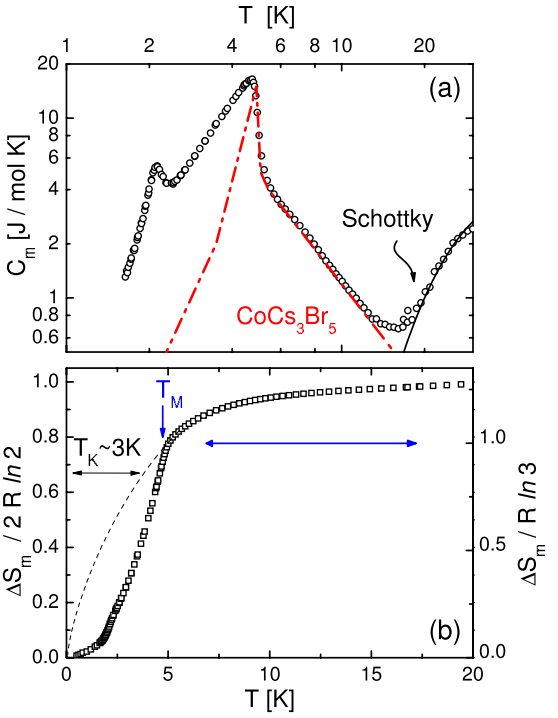

FIG. 6. (Color online) (a) Comparison of measured specific heat tail at $T>T_M$ with the exemplary two-dimensional system $CoCs_3Br_5$ (Ref. 21), see the text. Notice that one f.u. (i.e., one mol) involves two Ce atoms. (b) Comparison of thermal entropy gain between $2R\ln 2$ (left axis) and $R\ln 3$ (right axis) scales.

The fact that, in comparison with $CoCs_3Br_5$ the $C_m(T)$ of Ce_2Pd_2Sn is computed as "per mol" (i.e., =2Ce atoms), and that the reference compound has an effective spin $\mathbb{S}_{eff}=1$, provide the keys to understanding the physics of this compound since both properties suggest the formation of magnetic dimers built up through the J_1 interaction. Since the $\mathbb{S}_{eff}=1$ momentum has three quantum projections, the measured entropy has to increase accordingly. In fact, the 80% of $\Delta S_m=2R\ln 2$ collected up to $T=T_M$ corresponds to $R\ln 3$, as depicted on the right axis of Fig. 6(b). Since for $T>T_M$, the Ce-F dimers revert to individual Ce atoms, remanent entropy is related to the entropy relaxed in the $C_m(T>T_M)$ tail according to the $(2\ln 2-\ln 3)/2\ln 2$ difference.

The consequent structural loci of those dimers in a square lattice is sketched in Fig. 5(a), where the $\mathbb{S}_{eff}=1$ moments are depicted in the center of the $d_{\text{Ce-1Ce}}$ spacing as ⊙. This structural configuration of dimers is topologically equivalent to the Shastry-Sutherland systems[24] proposed for AF dimers and interdimer interactions, i.e., AF J_1 and J'. As it was pointed out by theoretical calculations.[25] Such a combination of interactions can lead to a stable AF-GS, recently realized in Yb_2Pt_2Pb single crystals,[26] which undergoes a slight shift of Pt atoms that results in two kinds of Yb-Pt tetrahedra.

Comparing these Yb and Ce isotypic compounds, we can note the heavy fermion character of Yb_2Pt_2Pb, with $\gamma = 311$ mJ/mol K^2,[26] whereas the Ce one shows a record low value of $\gamma = 7$ mJ/mol K^2. The hybridization effect may explain the lower entropy value of Yb_2Pt_2Pb at $T = T_N[\Delta S_m(T_N) = 0.58R \ln 2]$ compared with that of $Ce_2Pd_2Sn[\Delta S_m(T_M) = 0.80R \ln 2]$. Among the similarities, one can mention the similar CF splitting of the first excited level ($\Delta_1 = 70$ and 65 K, respectively), though their $1/\chi(T)$ curves show opposite signs. In both compounds, the extended tails above their respective upper transitions become significant at about three times $T_N(T_M)$. At lower temperatures, they show an anomaly at nearly one half of the upper transition. Worth noting is the fact that, while in Yb_2Pt_2Pb it looks like a shoulder [see Fig. 5(b) in Ref. 26], it is a first-order transition in Ce_2Pd_2Sn.

Since in the compound under study J_1 is ferromagnetic, and that situation was not proved theoretically to become a stable GS, our magnetic scenario seems to be nontrivial or perhaps even metastable. Furthermore, taking into account the modulated character of the intermediate phase, an AF interaction between dimers [i.e., J' in Fig. 5(c)] can be expected. Particularly, in the case of Ce_2Pd_2Sn, the low-temperature magnetic properties suggest that the proposed Ce-Ce magnetic dimerization arises once ΔS_m becomes $< R \ln 2$ [at $T \leq 20$ K as suggested in Fig. 6(a)] when the paramagnetic degrees of freedom of the doublet GS start to condense. Coincidentally, the straight line extrapolating $1/\chi$ to $\theta_P^{LT} = 4.4$ K is well defined up to that temperature. However, when those dimers start to interact AF to each other via J' [as expected from the cusp of $M(T)$ at T_M], the long-range order parameter cannot stabilize in a simple manner. Notice that only the coupling between nn dimers is depicted in Fig. 5(c) for simplicity, while the Hamiltonian proposed in Ref. 25 involves a set of nnn couplings. This apparent intrinsic instability of the intermediate phase (probably originated in frustration effects) ends at the lower transition $T_C = 2$ K, where a three-dimensional (3D) F-GS takes over.

IV. CONCLUSIONS

These experimental results confirm Ce_2Pd_2Sn as one of the scarce examples of ferromagnetic ground state among Ce intermetallics, with very stable magnetic moments and practically no traces of Kondo effect in the ground and excited CF states.

At intermediate temperatures ($T < 20$ K) magnetic interactions develop with an excitation spectrum mimicking a quasi-two-dimensional square lattice $S_{eff} = 1$ model. This property, the entropy value at $T_M[\Delta S_m(T_M) = R \ln 3]$, and the structural morphology suggest the progressive formation of Ce-Ce ferromagnetic dimers within a pattern resembling that proposed by Shastry-Sutherland. The F character of J_1 is recognized from the positive value of θ_P^{LT} and the entropy related to a threefold degenerate state, whereas the AF character of the exchange J' between dimers explains the cusp of $M(T)$ at $T_M = 4.8$ K. Nevertheless, this interaction is not able to stabilize the intermediate phase ($T_M \geq T \geq T_C$) leading the system to another phase transition.

The comparison with isotypic Yb_2Pt_2Pb and model predictions suggests that no stable GS is reached in a combination of F dimers (J_1) and AF exchange (J') among them, at least in this intermetallic compound. Nevertheless, an exotic phase with a nontrivial order parameter compete in energy within a short range of temperature till the 3D F-GS takes over. At the Curie temperature $T_C = 2.1$ K a first-order transition is observed in $C_P(T)$, $\rho(T)$, and χ_{ac}, including hysteretic features. Below T_C, the $C_P(T)$ dependence reveals a gap of anisotropy $E_g \approx 7$ K in the spectrum of magnons.

Further measurements are in progress to investigate the magnetic phase diagram of Ce_2Pd_2Sn and the effect of a slight deviation from stoichiometry.

ACKNOWLEDGMENTS

We are grateful to C. Geibel and M. Giovannini for clarifying discussions, and to K. Ogando for her participation in magnetic measurements. This work was partially supported by PIP-6016 (CONICET) and Secyt-UNC project 6/C256. J.G.S. and M.G.B. are members of the Consejo Nacional de Investigaciones Científicas y Técnicas and Instituto Balseiro (UN Cuyo) of Argentina.

[1] E. Bauer, G. Hilscher, H. Michor, Ch. Paul, Y. Aoki, H. Sato, D. T. Adroja, J.-G. Park, P. Bonville, C. Godart, J. Sereni, M. Giovannini, and A. Saccone, J. Phys.: Condens. Matter **17**, S999 (2005).

[2] F. Hulliger, J. Alloys Compd. **221**, L11 (1995).

[3] M. Giovannini, H. Michor, E. Bauer, G. Hilscher, P. Rogl, T. Bonelli, F. Fauth, P. Fischer, T. Herrmannsdorfer, L. Keller, W. Sikora, A. Saccone, and R. Ferro, Phys. Rev. B **61**, 4044 (2000).

[4] M. N. Peron, Y. Kergadallan, J. Rebizant, D. Meyer, S. Zwirner, L. Havela, H. Nakotte, J. C. Sprilet, G. M. Kalvius, E. Colineau, J. L. Oddou, C. Jeandey, and J. P. Sanchez, J. Alloys Compd. **201**, 203 (1993).

[5] R. A. Gordon, Y. Ijiri, C. M. Spencer, and F. J. DiSalvo, J. Alloys Compd. **224**, 101 (1995).

[6] D. Kaczorowski, P. Rogl, and K. Hiebl, Phys. Rev. B **54**, 9891 (1996).

[7] F. Fourgeot, P. Gravereau, B. Chevalier, L. Fournes, and J. Etourneau, J. Alloys Compd. **238**, 102 (1996).

[8] D. Laffargue, F. Fourgeot, F. Bouree, B. Chevalier, T. Roisnel, and J. Etourneau, Solid State Commun. **100**, 575 (1996).

[9] A. Braghta, G. Schmerber, A. Derory, J. G. Sereni, and J. P. Kappler, J. Magn. Magn. Mater. **320**, 1141 (2008).

[10] R. A. Gordon and F. J. DiSalvo, J. Alloys Compd. **238**, 57 (1996).

[11] J. G. Sereni, T. Westerkamp, R. Kuchler, N. Caroca-Canales, P. Gegenwart, and C. Geibel, Phys. Rev. B **75**, 024432 (2007).

[12] J. G. Sereni, P. Pedrazzini, E. Bauer, A. Galatanu, Y. Aoki, and H. Sato, J. Phys.: Condens. Matter **18**, 3789 (2006).

[13] J. C. Gomez-Sal, J. Rodriguez Fernandez, R. J. Lopez Sánchez, and D. Gignoux, Solid State Commun. **59**, 771 (1986).
[14] A. I. Akhiezer, V. G. Bar'yakhtar, and S. V. Peletminskii, in *Spin Waves*, North-Holland Series in Low Temperature Physics, edited by C. J. Gorter (North-Holland, Amsterdam, 1968), Vol. I, Chap. 6, p. 201.
[15] J. P. Kappler, M. J. Besnus, P. Lehmann, A. Meyer, and J. G. Sereni, J. Less-Common Met. **111**, 261 (1985).
[16] L. J. Suntröm, in *Handbook for Physics and Chemistry of Rare Earths*, edited by K. A. Gschneidner, Jr. and L. Eyring (North-Holland, Amsterdam, 1978), Vol. 1, Chap. 5.
[17] See, e.g., S. N. de Medeiros, M. A. Continentino, M. T. D. Orlando, M. B. Fontes, E. Baggio-Saitovitch, A. Rosch, and A. Eichler, Physica B **281-282**, 340 (2000); M. A. Continentino, S. N. de Medeiros, M. T. D. Orlando, M. B. Fontes, and E. M. Baggio-Saitovitch, Phys. Rev. B **64**, 012404 (2001).
[18] J. G. Sereni, Physica B **215**, 273 (1995).
[19] See, for example, J. G. Sereni, in *Handbook for Physics and Chemistry of Rare Earths*, edited by K. A. Gschneidner, Jr. and L. Eyring (Elsevier Science BV, Amsterdam, 1991), Vol. 15, Chap. 98.
[20] R. Kiessling, Acta Chem. Scand. (1947-1973) **4**, 209 (1950).
[21] R. F. Wielinga, H. W. Blöte, J. A. Roest, and W. J. Huiskamp, Physica (Amsterdam) **34**, 223 (1967).
[22] See, e.g., J. G. Sereni, in *Encyclopedia of Materials, Science Technology*, edited by K. H. Buschow and E. Gratz (Elsevier Science, New York, 2001), Vol. 5, p. 4986.
[23] H.-U. Desgranges and K. D. Schotte, Phys. Lett. **91A**, 240 (1982).
[24] B. S. Shastry and B. Sutherland, Physica B & C **108**, 1069 (1981).
[25] S. Miyahara and K. Ueda, Phys. Rev. Lett. **82**, 3701 (1999).
[26] M. S. Kim, M. C. Bennett, and M. C. Aronson, Phys. Rev. B **77**, 144425 (2008).